

Article

Inducing β Phase Crystallinity in Block Copolymers of Vinylidene Fluoride with Methyl Methacrylate or Styrene

Nahal Golzari ¹, Jörg Adams ² and Sabine Beuermann ^{1,*}

¹ Institute of Technical Chemistry, Clausthal University of Technology, Arnold-Sommerfeld-Strasse 4, 38678 Clausthal-Zellerfeld, Germany; nahal.golzari@tu-clausthal.de

² Institute of Physical Chemistry, Clausthal University of Technology, Arnold-Sommerfeld-Strasse 4, 38678 Clausthal-Zellerfeld, Germany; adams@pc.tu-clausthal.de

* Correspondence: sabine.beuermann@tu-clausthal.de; Tel.: +49-532-372036

Received: 20 June 2017; Accepted: 20 July 2017; Published: 26 July 2017

Abstract: Block copolymers of poly(vinylidene fluoride) (PVDF) with either styrene or methyl methacrylate (MMA) were synthesized and analyzed with respect to the type of the crystalline phase occurring. PVDF with iodine end groups (PVDF-I) was prepared by iodine transfer polymerization either in solution with supercritical CO₂ or in emulsion. To activate all iodine end groups Mn₂(CO)₁₀ is employed. Upon UV irradiation Mn(CO)₅ radicals are obtained, which abstract iodine from PVDF-I generating PVDF radicals. Subsequent polymerization with styrene or methyl methacrylate (MMA) yields block copolymers. Size exclusion chromatography and NMR results prove that the entire PVDF-I is converted. XRD, FT-IR, and differential scanning calorimetry (DSC) analyses allow for the identification of crystal phase transformation. It is clearly shown that the original α crystalline phase of PVDF-I is changed to the β crystalline phase in case of the block copolymers. For ratios of the VDF block length to the MMA block length ranging from 1.4 to 5 only β phase material was detected.

Keywords: fluoropolymers; vinylidene fluoride; block copolymers; crystallization; phase separation

1. Introduction

Most hydrofluorocarbon polymers show extraordinary thermal stability, chemical inertness, and weatherability, as well as being stable against various types of radiation. Large scale applications encompass, e.g., coatings, membranes, tubes, and piping equipment [1,2] Poly(vinylidene fluoride) (PVDF) is special, because additionally it shows ferro-, piezo-, and pyroelectric properties [3–10]. These electroactive properties are associated with the all trans conformation β crystalline phase of PVDF. However, the semi-crystalline polymer forms not only β phase material, but four more polymorphs (α , γ , δ , and ϵ phase) which are known [11,12].

The α polymorph is the most readily available phase. Several processes were reported to obtain β phase material, such as ultrafast cooling, melting under high pressure, mechanical stretching of the α polymorph, and blending with poly(methyl methacrylate) (PMMA), BaTiO₃ or palladium. An excellent overview on the various phases of PVDF and applications as electroactive materials is presented in reference [13]. In addition to the homopolymer of vinylidene fluoride (VDF), in binary and ternary copolymers of VDF with trifluoroethylene and chlorotrifluoroethylene β phase formation is found [3,14,15]. Due to higher sterical hindrance compared to VDF homopolymers the formation of the all trans β phase is preferred [13].

Frequently, blends of PVDF and PMMA are considered for β phase formation [16] due to favorable interactions between the highly electronegative F atoms in PVDF and the carbonyl groups of PMMA. Moreover, steric reasons are supposed to favor the trans conformation of both polymers and may lead

to a chain extension and consequently β crystallinity is promoted [16]. In addition, the influence of the glass transition temperature, T_g , on the relative growth rates of α and β spherulites is discussed [16]. Depending on polymer molecular weights and the ratio of both polymers in the blend, phase separation may occur. If phase separation in polymer blends induces β phase crystallinity of the PVDF domains, it appears particularly interesting to consider block copolymers consisting of one PVDF block. Again, phase separation is expected to occur and β phase crystallinity should occur.

So far the number of reports on PVDF block copolymers is still rather small. Reversible deactivation transfer polymerizations frequently used for block copolymer synthesis of styrene and many (meth)acrylate monomers are difficult to be performed with VDF, mainly due to the highly reactive primary propagating radical. Methods involving degenerative chain transfer constitute an exception from the above said. Iodine transfer polymerizations (ITP) [17–20], the use of xanthates [21–24] or reversible addition fragmentation transfer (RAFT) polymerizations [25,26] allow for good control of molecular weights, result in low dispersities, and may yield block copolymers.

Generally, in ITP perfluorinated alkyl iodides such as $C_6F_{13}I$ or $C_6F_{12}I_2$ are used as chain transfer agents [19,20]. Due to the rather low bond energy between iodine and the propagating chain, the transfer reaction of iodine is reversible. Regular head to tail addition leads to $-(CF_2-CH_2)-$ motifs in the polymer chain. Further, tail to tail, tail to head, and head to head additions play an important role in VDF polymerizations leading to $-CF_2-CH_2-CH_2-CF_2-$ and $-CH_2-CF_2-CF_2-CH_2-$ sequences in the polymer chains as well as $-CH_2-CF_2-I$ and $-CF_2-CH_2-I$ end groups as identified by NMR spectroscopy. $-CH_2-CF_2-I$ is at least 25 times more active than $-CF_2-CH_2-I$ [27]. As a consequence, the fraction of inactive $-CF_2-CH_2-I$ chain ends increases with conversion. Previously, the active species, $-CH_2-CF_2-I$, was used for follow-up reactions [28–30]. In all cases, only the polymer with active end groups was used.

Asandei and coworkers reported a synthetic strategy using $Mn_2(CO)_{10}$ for activation of both iodine polymer end groups, consequently allowing for an efficient transformation of all polymer chains [31–33]. Since the linkage between two Mn atoms is weak (20–40 kJ) [34,35], visible light allows for the production of two $\bullet Mn(CO)_5$ metalloradicals with good quantum efficiency [36]. $\bullet Mn(CO)_5$ radicals being very good halide abstractors irreversibly activate both iodine end groups originating from ITP and $Mn(CO)_5-I$ is formed [31]. Both radicals obtained ($-CF_2\bullet$ and $-CH_2\bullet$) may react with an added monomer to initiate a free radical polymerization leading to block copolymers where PVDF-I serves as a macroinitiator.

A different synthetic strategy is the preparation of block copolymers via functional benzoyl peroxide initiated polymerization of VDF and subsequent synthesis of the second block using atom transfer radical polymerization or ring opening polymerization [37–39]. For example, the resulting block copolymers with the second block being poly(butyl methacrylate) showed β phase crystallinity of the PVDF block with a molecular weight of around $15,000 \text{ g}\cdot\text{mol}^{-1}$ and a PVDF molar content of around 0.5.

Due to the above mentioned favorable interactions and the associated miscibility of PMMA and PVDF, in this contribution the synthesis of block copolymers of VDF with MMA is reported. In addition, some copolymers with styrene as the second monomer were prepared. Firstly, PVDF-I was synthesized by ITP in supercritical carbon dioxide as solvent [40,41] or in emulsion [42]. Then, with PVDF-I as macroinitiator $Mn_2(CO)_{10}$ -photomediated free radical polymerization with MMA or styrene were carried out to yield well-defined block copolymers. The molecular weight of the initial PVDF macroinitiator and the ratio of the block lengths was varied. Atomic Force Microscopy (AFM) of thin films is considered to identify phase separation of both polymer blocks. In order to identify whether the PVDF domains are crystalline and to analyze which type of crystalline phase is determined, Fourier transform infrared spectroscopy (FTIR), X-ray powder diffraction (XRD), and differential scanning calorimetry (DSC) were used.

2. Methods and Materials

2.1. Materials

Vinylidene fluoride (VDF, Dyneon GmbH, Burgkirchen a.d.Alz, Germany, 99.5%), styrene (S, Sigma-Aldrich, Taufkirchen, Germany, 99.5%), methyl methacrylate (MMA, Sigma-Aldrich, Taufkirchen, Germany, 99%), di-*tert*-butylperoxide (DTBP, Merck, Darmstadt, Germany, 98%), 1-iodoperfluorohexane (ABCR, Karlsruhe, Germany, 99%), 1,4-diiodooctafluorobutane (Dyneon GmbH, Burgkirchen a.d.Alz, Germany), dimanganese decacarbonyl (Sigma-Aldrich, Taufkirchen, Germany, 98%), methanol (95%), hydrochloric acid (37%), *N,N*-dimethyl acetamide (DMAc, Acros, Geel, Belgium, 99%), ammonium 4,8-dioxa-3*H*-perfluorononanoate (Dyneon, GmbH, Burgkirchen a.d.Alz, Germany), ammonium peroxydisulfate (Fluka, Honeywell, Hannover, Germany, $\geq 98.0\%$), carbon dioxide (Air Liquide, Paris, France, 99.8%), *N,N*-dimethylformamide- d_7 (Deutero GmbH, Kastellaun, Germany, 99.5%), and acetone- d_6 (Deutero GmbH, Kastellaun, Germany, 99.8%) were used as received.

2.2. Characterization

To characterize the polymers, the following techniques and equipment were used. Size-exclusion chromatography (SEC) measurements were carried out at a column temperature of 45 °C using DMAc, which contains 0.1% LiBr as eluent. The SEC set-up consists of an Agilent 1200 isocratic pump, an Agilent 1200 refractive index detector, and four PSS GRAM columns (Guard, 100 Å, 3000 Å, and 3000 Å) from Polymer Standard Service (PSS). Measurements were carried out at a flow rate of 1 mL·min⁻¹. Polystyrene standards (PSS) were used for calibration. For FT-IR measurements a Vertex 70 Bruker spectrometer (Bruker Optik GmbH, Bremen, Germany) equipped with a global source and a photoacoustic cell (PA301) was used. Spectra were measured with a resolution of 4 cm⁻¹. ¹H and ¹⁹F NMR spectra of the polymers were recorded on a Bruker AVANCE 400 MHz spectrometer at room temperature. Acetone- d_6 and also *N,N*-dimethylformamide- d_7 were used as solvents. To characterize the phase separation of the copolymers, thin polymer films were prepared either by casting a solution directly onto clean mica or by spin coating onto the same substrate (5 mg polymer in 1 mL DMAc, spin-coater WS-650MZ, Laurell, North Wales, PA, USA). These films were analyzed with an AFM (extended multimode, NanoScope IIIa controller, Veeco/Digital Instruments, Plainview, NY, USA) operating in tapping mode at room temperature in air. To selectively etch the PMMA or PS blocks while keeping the PVDF intact, air-plasma generated in a RF plasma cleaner (PDC-32G, Harrick-Plasma, Ithaca, NY, USA) was used for up to 60 s. This technique has been used successfully to contrast PS in PMMA-PS block copolymers [43]. XRD analyses at KIT were conducted by a STADI MP diffractometer (STOE, Darmstadt, Germany) with Ge-monochromatized Cu-K α radiation ($\lambda = 1.54060$ Å). The XRD measurements at TUC were conducted with Cu-K α (graphite monochromator) as well. A Bruker AXS D8 Discover diffractometer was used, equipped with a General Area Diffraction System (GADDS, Bremen, Germany) as detector. DSC measurements were performed with a DSC 1/500658/200W STARe system by Mettler Toledo, Columbus, OH, USA. This system is equipped with a FRS5 sensor and liquid nitrogen cooling. Each sample passes through a complete heating and cooling cycle before the second heating run is used for analysis. The heating or cooling rate is 10 °C·min⁻¹ for all measurements.

2.3. Synthesis of PVDF-I

Polymers with iodine end group (PVDF-I) were synthesized by iodine transfer polymerization (ITP). C₆F₁₃I was used as the chain transfer agent, DTBP as the initiator, and CO₂ as the solvent. A typical experiment was performed at a constant temperature of 120 °C and an initial pressure of 1500 bar. During polymerization the pressure decreased to around 850 bar due to volume contraction upon consumption of the gaseous monomer. To produce PVDF homopolymers with a number average molecular weight, M_n , between 1500 and 2500 g·mol⁻¹, a weight fraction of VDF of around 70%,

1.5 g DTBP (10.4 mmol, $c = 0.076 \text{ mol}\cdot\text{L}^{-1}$), and 8.0 g $\text{C}_6\text{F}_{13}\text{I}$ (1.8 mmol, $c = 0.13 \text{ mol}\cdot\text{L}^{-1}$) were used. PVDF-I with $M_n > 10^4 \text{ g}\cdot\text{mol}^{-1}$ was obtained from reactions with reduced quantities of initiator and chain transfer agent: 0.75 g DTBP (5.1 mmol, $c = 0.056 \text{ mol}\cdot\text{L}^{-1}$) and 4.0 g $\text{C}_6\text{F}_{13}\text{I}$ (9.0 mmol, $c = 0.097 \text{ mol}\cdot\text{L}^{-1}$) were used. The preparation of the reaction mixture, the polymerization procedure, and the reaction set-up were detailed elsewhere [40].

I-PVDF-I used for samples 2 and 3 is synthesized by emulsion polymerization. The reaction was performed at 90 °C and 15 bar for 4 h. Ammonium 4,8-dioxa-3H-perfluorononanoate was used as the surfactant ($0.022 \text{ mol}\cdot\text{L}^{-1}$), ammonium peroxydisulfate as the initiator ($6 \text{ mmol}\cdot\text{L}^{-1}$) and $\text{C}_4\text{F}_8\text{I}_2$ as the chain transfer agent ($12 \text{ mmol}\cdot\text{L}^{-1}$) [42].

The number average molecular weights M_n and dispersities of the PVDF homopolymers are listed in Table 1. It should be noted that M_n data refers to SEC calibration with polystyrene standards. In order to estimate absolute molecular weights the principle of universal calibration was applied [44]. With Mark-Houwink parameters K and a being known for polystyrene and for PVDF in dimethyl acetamide as eluent [45], M_n values are derived, which are about 15% lower than the M_n values listed in Table 1. Since the K and a values were derived from a higher molecular weight sample, and since SEC is generally considered to be associated with an uncertainty of 10% to 15%, we decided on listing the data derived from the primary experimental data.

2.4. Synthesis of the Block Copolymers (PVDF-*b*-PMMA and PVDF-*b*-PS)

In a round-bottom flask, 100 mg of PVDF-I (or I-PVDF-I), 1 mL of the other monomer (MMA, 9.4 mmol or styrene 9.1 mmol) and 36 mg of $\text{Mn}_2(\text{CO})_{10}$ (0.092 mmol) were dissolved in 2 mL DMAc. In addition, reactions with different amounts of the monomers (see Table 1) were carried out. The mixture was purged with N_2 for 10 min, then placed in an oil-bath, and stirred at 90 °C under visible light irradiation (Oriol 60006 lamp, LOT group, Darmstadt, Germany) for 1 h. As suggested by Asandei and coworkers [31], the polymer was precipitated in acidic methanol, filtered, and dried.

3. Results and Discussion

ITP of VDF with perfluorinated alkyl iodides serving as chain transfer agents lead to polymers with the following two end groups: $-\text{CF}_2-\text{CH}_2-\text{I}$ and $-\text{CH}_2-\text{CF}_2-\text{I}$ [27]. As reported by Asandei and coworkers, the $\bullet\text{Mn}(\text{CO})_5$ radical obtained upon UV irradiation of $\text{Mn}_2(\text{CO})_{10}$ may abstract I from both chain ends [31]. In the following the PVDF chain extension and block copolymer synthesis based on the use of $\text{Mn}_2(\text{CO})_{10}$ is described.

3.1. Chain Extension of PVDF

For block copolymer synthesis PVDF samples with different molecular weights were used. In addition, the amount of macroinitiator and comonomer were varied. Details are displayed in Table 1. In every case, 36 mg of $\text{Mn}_2(\text{CO})_{10}$, 2 mL of DMAc and a reaction time of 1 h were chosen. The results of PVDF macroinitiator and copolymer SEC analyses as well as copolymer compositions derived from NMR analyses are also listed in Table 1.

Samples 2 and 3 were obtained with identical amounts of macroinitiator I-PVDF-I and different amounts of MMA. As expected, the higher MMA concentration leads to significantly higher block copolymer molecular weights. Samples 1, 4, and 5 show that variation of PVDF molecular weight at otherwise identical conditions leads to block copolymers with significantly enhanced molecular weights, while dispersities are slightly lower than for the macroinitiator.

In order to test for the formation of block copolymers the molecular weight distributions (MWDs) are considered. While SEC does not give any information on the absolute molecular weights and block lengths due to calibration relative to polystyrene, the position of the MWDs provides information on the chain extension. As an example, Figure 1 gives the MWDs of the macroinitiator and a copolymer containing PMMA as the second block. The block copolymer MWD is clearly shifted to higher

molecular weight compared to the MWD of the PVDF-I macroinitiator, which indicates a successful chain extension.

Table 1. Details of block copolymer synthesis and resulting block copolymers properties with the amount of macroinitiator m_{PVDF} , the volume of comonomer V_{co} , molecular weights ($M_{\text{n,block}}$), dispersities (D_{block}), molar ratio of VDF and comonomer ($n_{\text{VDF}}/n_{\text{co}}$), and volume fraction of the comonomer in the copolymer. $M_{\text{n,PVDF}}$ and D_{PVDF} refer to the PVDF-I^a or I-PVDF-I^b macroinitiator. The SEC was calibrated with polystyrene. In all cases 36 mg $\text{Mn}_2(\text{CO})_{10}$, 2 mL DMAc and a reaction time of 1 h were chosen.

No.	$M_{\text{n,PVDF}}/\text{g}\cdot\text{mol}^{-1}$	D_{PVDF}	$m_{\text{PVDF}}/\text{mg}$	Comonomer	V_{co}/mL	$M_{\text{n,block}}/\text{g}\cdot\text{mol}^{-1}$	D_{block}	$n_{\text{VDF}}/n_{\text{co}}$	n_{VDF}	n_{co}	φ_{co}
1 ^a	2033	1.5	100	MMA	1	22,344	1.6	1/3	27	81	0.84
2 ^b	4344	2.0	100	MMA	0.5	15,176	1.6	1/0.83	58	48	0.64
3 ^b	4344	2.0	100	MMA	4	40,524	1.8	1/4	58	232	0.87
4 ^a	4518	1.4	100	MMA	1	39,450	1.8	1/2.3	60	138	0.85
5 ^a	11,500	1.4	100	MMA	1	50,520	1.7	1/0.67	153	102	0.58
6 ^a	11,500	1.4	100	MMA	0.2	12,080	1.5	1/0.21	153	33	0.33
7 ^a	11,500	1.4	100	MMA	0.5	36,170	1.3	1/0.37	153	57	0.46
8 ^a	11,500	1.4	100	MMA	1.5	60,880	2.1	1/0.84	153	128	0.66
9 ^a	2033	1.5	100	S	1	13,220	3.6	1/0.56	27	15	0.59
10 ^a	11,500	1.4	100	S	3	33,040	1.3	1/0.91	153	140	0.58
11 ^a	11,500	1.4	200	S	1	19,856	1.9	1/0.71	153	109	0.50
12 ^a	11,500	1.4	200	S	2	21,669	1.7	1/0.77	153	118	0.54

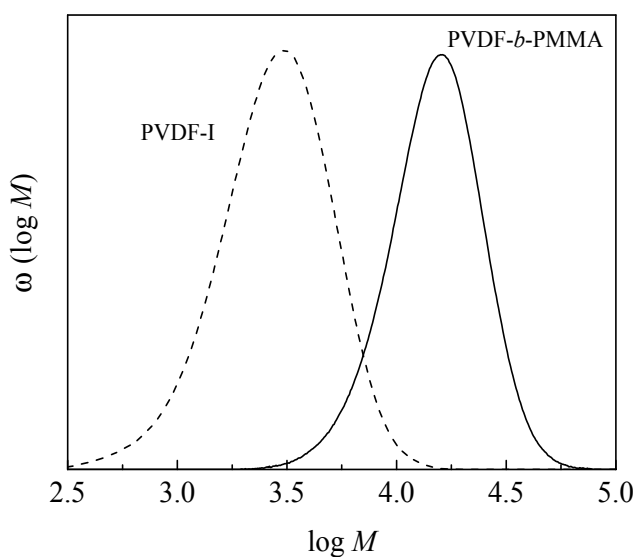


Figure 1. Molecular weight distributions poly(vinylidene fluoride) with iodine end groups (PVDF-I). PVDF-I (dashed) and resulting block copolymer with methyl methacrylate (MMA) (full, sample 1).

SEC elution chromatograms were analyzed to evaluate whether the entire PVDF-I macroinitiator was transformed. As an example, Figure 2 gives the SEC elution curves for PVDF-I with $M_{\text{n}} = 2033 \text{ g}\cdot\text{mol}^{-1}$ and the block copolymer sample 1. The negative peak assigned to PVDF-I occurs at an elution time of 31 min, whereas the chromatogram of the block copolymer does not show any contributions from PVDF-I at 31 min. The elution curves of all other copolymers listed in Table 1 show no peak originating from PVDF-I. Contrary to reference [31] where a reaction time of 5 h and a temperature of 110 °C were selected, here 1 h and 90 °C were sufficient for complete conversion of the macroinitiator. The difference is suggested to be due to differences in UV irradiation and consequently differences in the generation of $\bullet\text{Mn}(\text{CO})_5$ radicals.

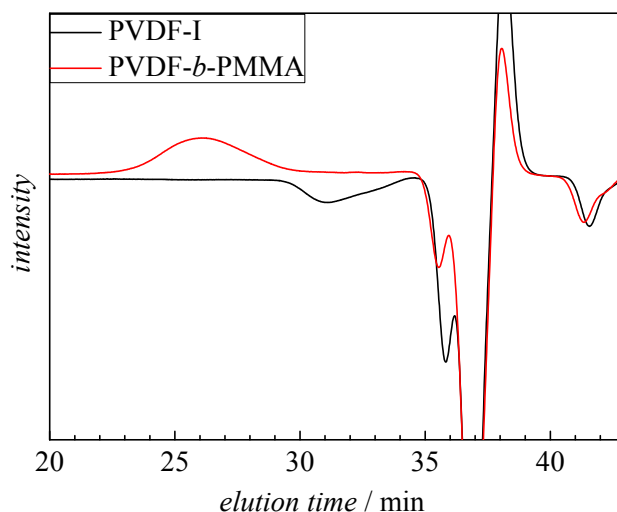


Figure 2. Elution curve of PVDF-I with $M_n = 2033 \text{ g}\cdot\text{mol}^{-1}$ and copolymer sample 1.

3.2. Block Copolymer Composition

Since the dispersities of PVDF-I and the block copolymer are rather close, it is anticipated that both chain ends, the $\text{CF}_2\text{-I}$ and the $\text{CH}_2\text{-I}$ end group, were transformed. To prove whether both end groups were activated and polymerized, end group analyses were carried out via ^1H and ^{19}F NMR spectroscopy. Firstly, a blank reaction of PVDF-I and $\text{Mn}_2(\text{CO})_{10}$ in the absence of comonomer is considered. The reaction was performed with 100 mg PVDF-I dissolved in 3 mL DMAc containing 36 mg of $\text{Mn}_2(\text{CO})_{10}$ (0.092 mmol) under UV irradiation at 40°C for 3 h. The PVDF radical formed was expected to abstract an H atom either from the solvent or from the polymer. Figure 3 shows ^1H NMR spectra of the original material (denoted PVDF-I) and PVDF obtained from the blank reaction (denoted PVDF-H). As expected PVDF-I shows both iodine end groups. According to reference [20] the peak at ~ 3.6 ppm is assigned to $-\text{CH}_2\text{-CF}_2\text{-I}$ and the peak at around 3.8 ppm refers to $-\text{CF}_2\text{-CH}_2\text{-I}$. Both peaks are only very weak in the spectrum of PVDF-H. Instead, a peak at about 6.3 ppm is found, which refers to $-\text{CH}_2\text{-CF}_2\text{-H}$ being due to transfer to solvent or polymer [46]. The red spectrum referring to PVDF-H also shows a peak at about 1.75 ppm, which represents $-\text{CF}_2\text{-CH}_3$ originating from $-\text{CF}_2\text{-CH}_2\text{-I}$ after replacing I with H [46]. The single peak at $\delta \sim 4.55$ ppm indicates the presence of $-\text{CH}_2\text{-CF}_2\text{-CH}=\text{CF}_2$ [31], which originates from termination via disproportionation. Peaks at $\delta \sim 2.19$ and 2.13 ppm represent the $-\text{CH}_2\text{-CF}_2\text{-CH}=\text{CF}_2$ motif. The strong peak at $\delta \sim 2.8\text{--}3.0$ ppm in both spectra refers to the $-\text{[CH}_2\text{-CF}_2\text{]}_n\text{-}$ head to tail PVDF sequence. The $-\text{CF}_2\text{-CH}_2\text{-CH}_2\text{-CF}_2\text{-}$ head to head PVDF sequence is associated with a peak at $\delta \sim 2.4$ which is however hardly seen in both spectra due to the very low M_n and consequently a small quantity of this sequence in the material. The acetone peak is seen around 2.05 ppm [46,47].

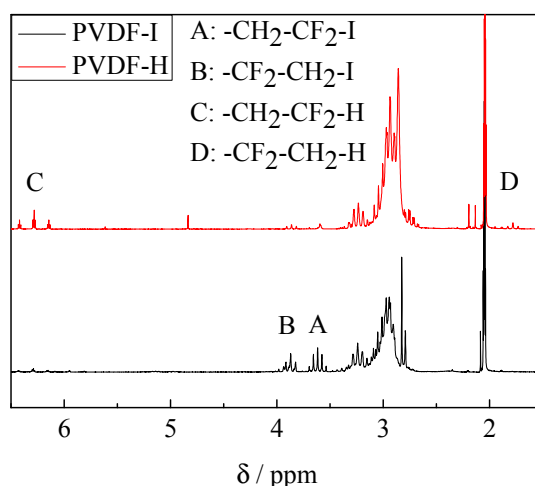


Figure 3. ¹H NMR spectra of PVDF-I (black) and PVDF-H (red).

The ¹H NMR spectrum in Figure 4 recorded for a block copolymer of VDF and MMA shows the expected peaks. The very strong peak at about 3.6 ppm is assigned to the $-\text{OCH}_3$ group of PMMA and two strong peaks between 0.8 and 1.2 ppm to the $-\text{CH}_3$ group at the main chain of PMMA. In addition, the above-mentioned peaks assigned to the methylene group of PVDF at 2.4 and 3.0 ppm are seen. Integration of the peak at $\delta \sim 3.6$ ppm for PMMA and at $\delta \sim 2.4$ and 3.0 ppm for PVDF allows for the calculation of the ratio of block lengths according to Equation (1).

$$\frac{n_{\text{PMMA}}}{n_{\text{PVDF}}} = \frac{\frac{1}{3} \int \text{CH}_3(3.6 \text{ ppm})}{\frac{1}{2} \int \text{CH}_2(3.0 \text{ ppm}) + \frac{1}{2} \int \text{CH}_2(2.4 \text{ ppm})} \quad (1)$$

The example in Figure 4 represents a block copolymer with n_{PVDF} to n_{PMMA} of 1 to 0.67 (sample 5). The results for all block copolymers are given in Table 1.

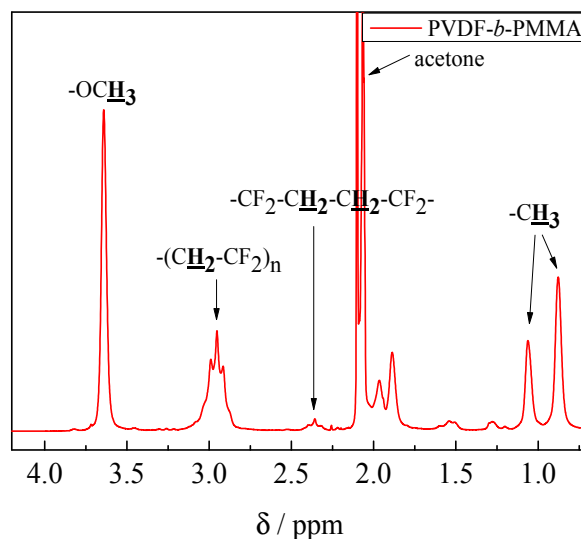


Figure 4. ¹H NMR spectrum of block copolymer sample 5.

The ¹H-NMR spectrum in Figure 5 recorded for a block copolymer consisting of VDF and styrene shows also the expected peaks. The strong peaks at around 6.6 to 7.2 ppm are assigned to the $-\text{C}_6\text{H}_5$

group of PS. Two other peaks at 1.94 ppm ($-\text{CH}_2-\underline{\text{CH}}-(\text{C}_6\text{H}_5)-$) and 1.63 ppm ($-\underline{\text{CH}_2}-\text{CH}-(\text{C}_6\text{H}_5)-$) also belong to PS. In addition, the peaks at 3.0 and 2.4 ppm assigned to the methylene groups in PVDF are seen. Integration of the peaks at 6.6 to 7.2 ppm for PS and at 2.4 and 3.0 ppm for PVDF allows for the calculation of the ratio of block lengths according to Equation (2).

$$\frac{n_{\text{PS}}}{n_{\text{PVDF}}} = \frac{\frac{1}{5} \int \text{C}_6\text{H}_5 (6.6 \text{ to } 7.2 \text{ ppm})}{\frac{1}{2} \int \text{CH}_2 (3.0 \text{ ppm}) + \frac{1}{2} \int \text{CH}_2 (2.4 \text{ ppm})} \quad (2)$$

The example in Figure 5 represents a block copolymer with n_{PVDF} to n_{PS} of 1 to 0.56. The results for all block copolymers containing styrene are listed in Table 1.

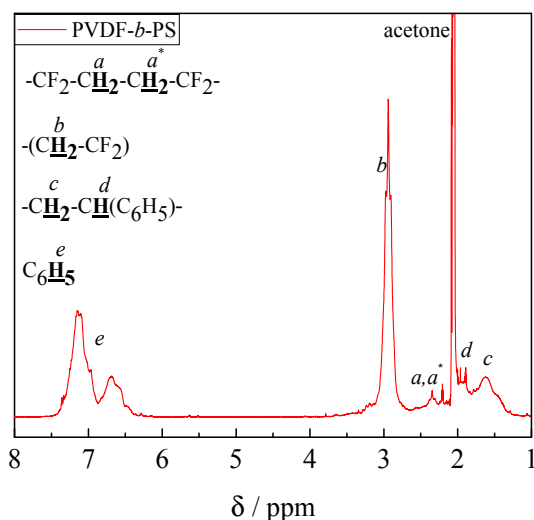


Figure 5. ^1H NMR spectrum of block copolymer sample 9.

The ^{19}F -NMR results also show that $-\text{CH}_2-\text{CF}_2-\text{I}$ and $-\text{CF}_2-\text{CH}_2-\text{I}$ chain ends of the PVDF macroinitiator were activated and polymerized. Peaks at $\delta \sim -38.4$ ppm and $\delta \sim -108$ ppm referring to $-\text{CH}_2-\text{CF}_2-\text{I}$ and $-\text{CF}_2-\text{CH}_2-\text{I}$ [31,47] respectively, of the macroinitiator clearly disappeared after copolymerization (see Figure S1 in Supporting Information).

3.3. Crystallinity of the Block Copolymers

To obtain additional information on the crystallinity of the products, FT-IR spectra were recorded. The FT-IR spectra of PVDF homopolymer and the block copolymers are given in Figure 6. One of the most prominent difference is the strong band at 1730 cm^{-1} , which is assigned to the carbonyl group in PMMA (blue spectrum) which is absent in the PVDF spectrum. In addition, the IR spectrum of the PMMA block copolymer shows a broad peak at 2951 cm^{-1} assigned to $-\text{OCH}_3$ of PMMA. The spectrum of the block copolymer with PS (red spectrum) shows the aromatic C-H stretching vibrations at 2850 , 2923 , 3025 , and 3060 cm^{-1} . The peaks at 1493 and 1062 cm^{-1} are assigned to the aromatic C-C bond stretching vibration. The absorbances at 3000 and 3100 cm^{-1} represent the C-C vibrations and peaks at 1151 cm^{-1} , as well as at 1193 cm^{-1} for C-F vibrations of the PVDF block [30,48]. The spectra clearly indicate the presence of both monomer units in the products.

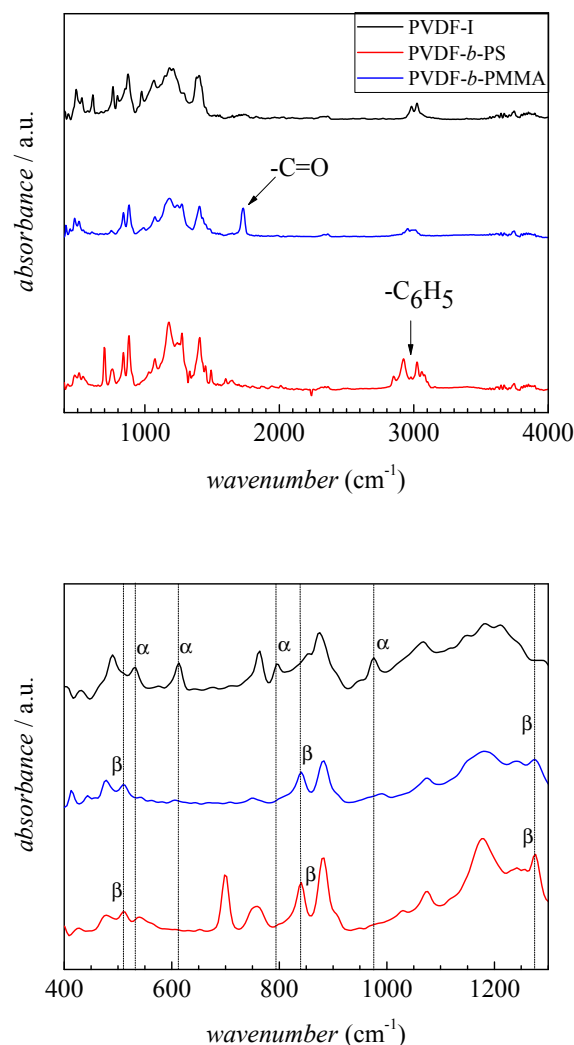


Figure 6. FT-IR results of PVDF-I (black), PVDF-*b*-PMMA (blue, sample 1), and PVDF-*b*-PS (red, sample 9). The vertical lines indicate peaks that are representative of either the α or β crystalline phase of PVDF.

To obtain information on the crystallinity of the PVDF block, the enlarged spectra in the wavenumber range from 500 to 1300 cm^{-1} depicted in the lower part of Figure 6 are considered. The spectrum of the PVDF-I macroinitiator shows distinct peaks at 532, 614, 795, and 976 cm^{-1} indicating the presence of α phase PVDF. On the contrary, the spectra of the block copolymers show none of the above mentioned peaks. New peaks at 510, 841, and 1276 cm^{-1} occur, which suggest the presence of β crystalline PVDF domains in the copolymer. Thus, the formation of PVDF-*b*-PMMA or PVDF-*b*-PS is suggested to be associated with a change in crystallinity of the PVDF segments.

The peak at 841 cm^{-1} in the IR spectrum may also be indicative of γ phase material, however, peaks at 776, 812, 833, and 1234 cm^{-1} also typical for the γ phase are not seen. As pointed out in literature, the flawless identification of β phase PVDF requires additional analyses such as XRD [13]. The results from XRD of PVDF-I and two block copolymers (sample 1 and 9 in Table 1) are depicted in Figure 7. The spectra are clearly different. The PVDF-I curve shows peaks at 2θ values of 17.66°, 18.30°, 19.90°, and 26.56°, which are related to the α phase [13]. On the other hand for the block copolymers only one peak with a maximum at around 20.26° is observed, which indicates the presence of β phase material. Peaks typical for the γ phase at 2θ values of 18.50°, 19.20° or 20.04° are not found [13]. Thus, the results from FT-IR and XRD strongly suggest the transformation of α to β phase PVDF domains in the copolymer. In addition, DSC analyses yield melting temperatures of 165 °C for the

block copolymers and 172 °C for the PVDF macroinitiator. These temperatures are characteristic for α and β phase material. Since γ phase PVDF is associated with melting temperatures between 180 and 190 °C [13] the presence of γ phase PVDF can be excluded.

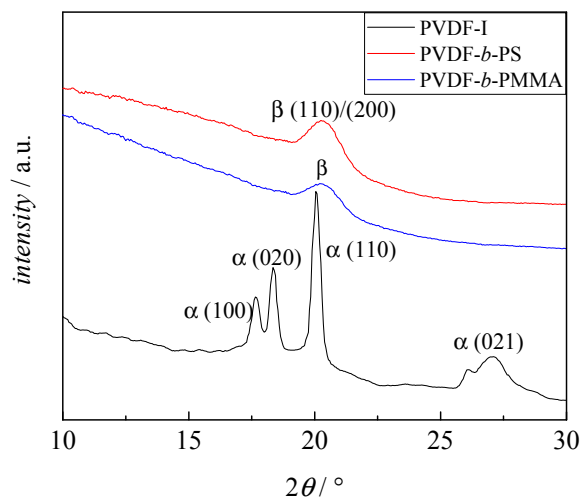


Figure 7. XRD results of PVDF-I (black), block copolymer with MMA (sample 4, blue) and block copolymer with styrene (sample 11, red).

The results demonstrate that the crystal structure of PVDF moieties is transformed from α to β after block copolymer synthesis. To identify which ratio of PVDF block length, n_{PVDF} , to comonomer block length, n_{co} , is required for this transformation a number of block copolymers was synthesized. For $n_{\text{PVDF}}/n_{\text{co}}$ ranging from 0.25 to 100 the characteristic IR peaks assigned to β phase material were found. In addition, contributions from α phase were observed. In cases where this ratio was between 1.4 and 5 exclusively the IR peaks indicative of β phase material were detected. With decreasing block length ratio $n_{\text{PVDF}}/n_{\text{co}}$ the fraction of crystalline material is reduced. In addition to the block length ratio, the absolute lengths of both blocks is important to be considered. The data presented here refer to PVDF segments with lengths between 27 and 153 monomer units. In future, longer PVDF segments need to be used as well.

According to references [16,48–50] the miscibility of PVDF and PMMA does not depend on temperature, which is attributed to interactions between the carbonyl group of PMMA and the dipole moment of PVDF as well as hydrogen bonding. Because of steric reasons, the above-mentioned interactions lead to an all trans conformation in both polymers. Further, the presence of MMA units may alter the glass transition temperature of PVDF, which affects the relative growth rates of α and β polymorphs [16].

According to dynamic mechanical measurements, pure PVDF may undergo four relaxations when frequency and temperature are changed [51,52]. One of these relaxations, which is associated with the glass transition may be shifted to higher frequencies and pressures after addition of PMMA. Essentially, PMMA facilitates relaxation from a lower energy level, which may be explained by breaking the interactions and correlations between the PVDF permanent moments in the amorphous-crystalline-interphase and improving the dielectric relaxation possibilities [16].

The piezoelectricity and pyroelectricity of PVDF are associated with the existence of a remnant polarization that is proportional to the degree of crystallinity [16]. PMMA, as the amorphous phase, surrounds individual crystallites, and therefore, affects the degree of crystallinity.

Figure 8 compares the XRD results of samples 6, 7, and 8 with PMMA volume fractions of 33%, 46%, and 66%, respectively, in the block copolymer. While it is clearly seen that no significant contributions from α phase are contained, a quantitative comparison of the XRD results of different samples is not feasible. However, the DSC results show that the integration of the melting peak and

the degree of crystallinity are proportional to block lengths ratio and volume fraction of PMMA in the block copolymer. In all cases, the integrals of the melting peak and the degree of crystallinity decrease, if the volume fraction of PMMA in the block copolymer increases.

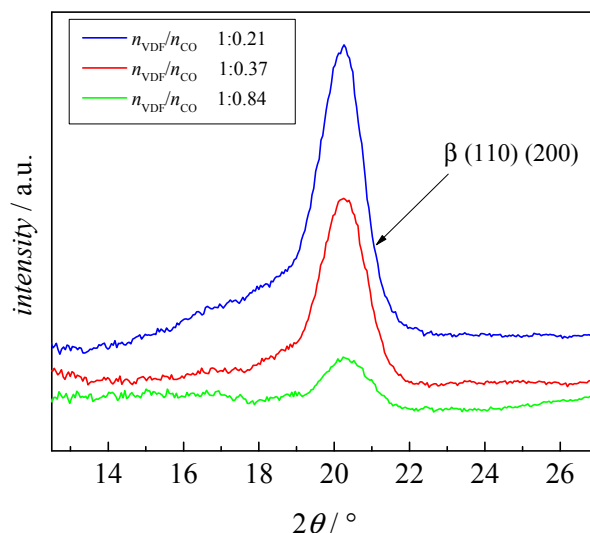


Figure 8. XRD curves for sample 6 (blue), 7 (red), and 8 (green) with the block length ratios as indicated.

Interestingly the block copolymers with PS as second block also show β phase crystallinity. The reason for this behavior is not yet clear. It may be suspected that the aromatic groups are directing the conformation to an all trans structure of PVDF. For low molecular weight species interactions between F atoms and for example aromatic rings were reported [53–56].

3.4. Phase Separation

To test for microphase separation of the two polymer blocks, AFM analyses of thin films of samples 4, 6, 10, and 11 obtained by spin coating on mica were carried out. Without selective etching of the PMMA or PS block by air-plasma, flat films were obtained that did not show any phase separation as indicated by the phase-image of the AFM (not shown). The phase-image contrasts in a semi-quantitative way differences in the material properties, e.g., hardness and viscoelasticity. After 10 s of air plasma treatment for every sample, a height variation in the topography image on the left hand side of Figures 9–12 is visible and the phase image on the right hand side of these figures shows small domains in a continuous matrix. These domains may be associated with a PVDF-rich microphase and the size of these domains scales with the volume fraction of PVDF in the copolymer. In Figures 9 and 10, it is notable that the continuous matrix in which the PVDF-domains are embedded covers a much smaller surface fraction in sample 6 compared to sample 4. This observation corresponds with the lower PMMA volume fraction of $\varphi_{CO} = 0.33$ in sample 6 compared to $\varphi_{CO} = 0.85$ in sample 4. Control experiments with blends of PMMA and PVDF homopolymers showed no phase separation.

AFM measurements at identical conditions were carried out for two copolymers with styrene blocks of different length (Figures 11 and 12). As expected, the size of the domains are proportional to the PVDF volume fraction in the copolymer. In Figure 12, it is notable that the continuous matrix containing the PVDF-domains covers a smaller surface fraction in sample 10 compared to sample 11 (Figure 11) because of the lower value of $\varphi_{CO} = 0.50$ compared to $\varphi_{CO} = 0.58$, respectively.

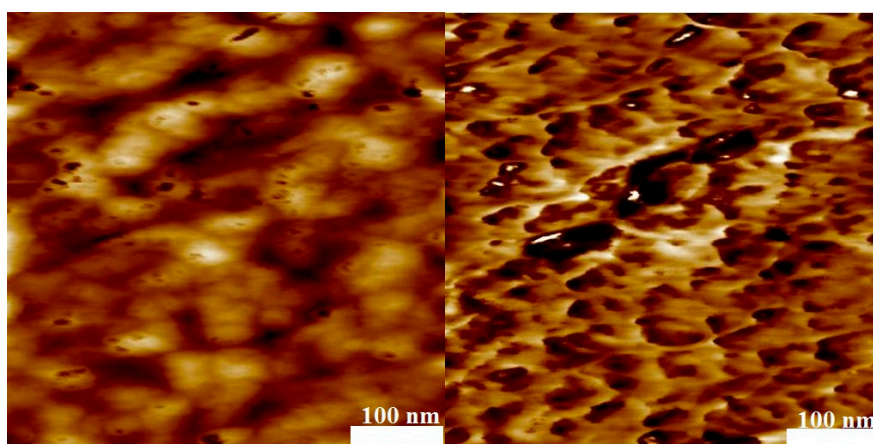


Figure 9. Atomic Force Microscopy (AFM) results of the block copolymer with MMA (sample 6) with $M_n = 12,080 \text{ g}\cdot\text{mol}^{-1}$ after 10 s of air-plasma treatment. Topography ((left) height scale: 5 nm) and phase image ((right) phase scale: 90°), Average domain size = 50 nm.

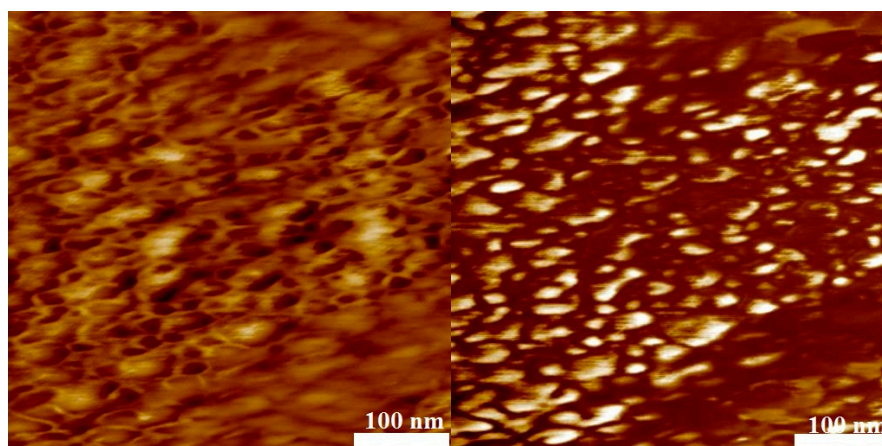


Figure 10. AFM results of the block copolymer with MMA (sample 4, $M_n = 39,450 \text{ g}\cdot\text{mol}^{-1}$) after 10 s of air plasma treatment. Topography ((left) height scale: 10 nm) and phase image ((right) phase scale: 50°), average domain size = 75 nm.

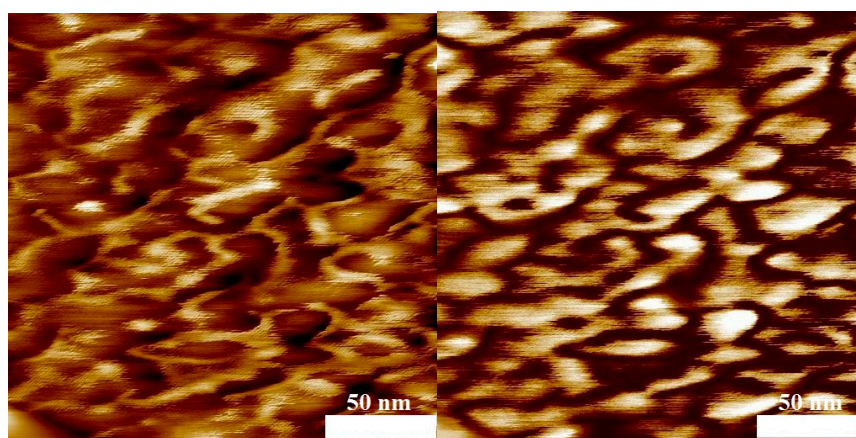


Figure 11. AFM results of the block copolymer with styrene (sample 11, $M_n = 19,856 \text{ g}\cdot\text{mol}^{-1}$) after 10 s of air-plasma treatment. Topography ((left) height scale: 10 nm) and phase image ((right) phase scale: 30°), average domain size = 80 nm.

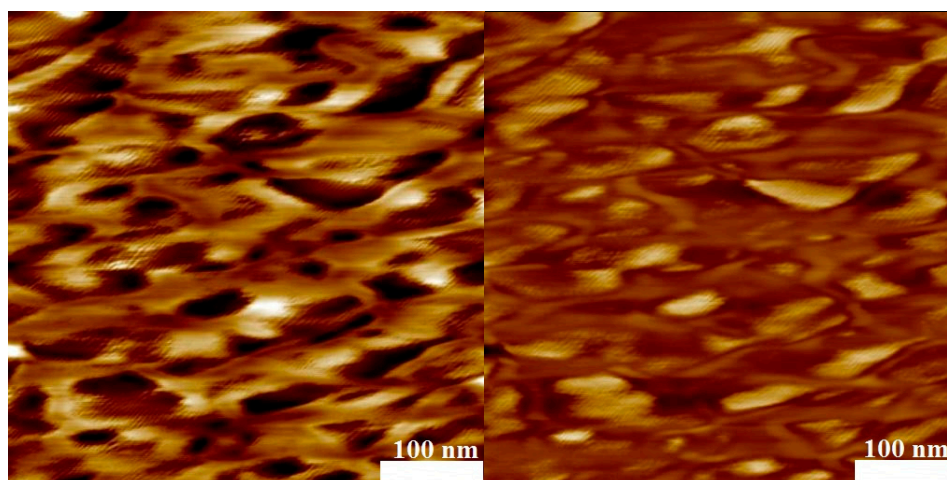


Figure 12. AFM results of the block copolymer with styrene (sample 10, $M_n = 33,040 \text{ g}\cdot\text{mol}^{-1}$) after 10 s of air-plasma treatment. Topography ((left) height scale: 10 nm) and phase image ((right) phase scale: 90°), average domain size = 120 nm.

4. Conclusions

PVDF-I obtained from iodine transfer polymerization served as macroinitiator for MMA and styrene polymerization. Due to four well-known propagation reactions in VDF polymerizations, two types of PVDF end groups were obtained: $\text{CF}_2\text{-CH}_2\text{-I}$ and $\text{CH}_2\text{-CF}_2\text{-I}$, which have very different reactivities. Following Asandei et al. the entire polymer material may be functionalized upon UV irradiation of $\text{Mn}_2(\text{CO})_{10}$ in the presence of PVDF-I [31]. $\bullet\text{Mn}(\text{CO})_5$ radicals obtained due to UV irradiation abstract iodine from both PVDF-I end groups. The resulting PVDF radicals initiate MMA and styrene free radical polymerizations leading to block copolymers of VDF and MMA or styrene, as indicated by SEC analyses and NMR spectra.

FTIR spectra suggest that the crystal phase is transformed from the α phase in case of PVDF-I to β phase PVDF-domains in case of the block copolymers. XRD measurements confirmed the transformation from α to β crystalline phase. Varying block length ratios $n_{\text{VDF}}/n_{\text{co}}$ from 0.25 to 100 resulted in β phase crystallinity. For ratios from 1.4 to 5 exclusively β phase material was detected. AFM results indicate a phase separation of the PVDF-segments from the other polymer, PMMA or PS. Mixtures of corresponding homopolymers do not show a distinct phase separation in the AFM images. The data indicates that the volume fraction of both monomer units within the block copolymers affects the structure formation.

Supplementary Materials: The following are available online at www.mdpi.com/2073-4360/9/8/306/s1, Figure S1: A comparison of ^{19}F NMR spectra of PVDF-I (blue) and the corresponding PVDF-*b*-PMMA (red, sample 1 in Table 1).

Acknowledgments: We are grateful to Dipl. Ing. Simone Wolff (Institute for Technical Thermodynamics and Refrigeration, Karlsruhe Institute of Technology (KIT)) for some of our XRD measurements. Florian Brandl is acknowledged for preparing I-PVDF-I by emulsion polymerization. We are thankful to Martina Heinz for the SEC and Ulrike Koecher for DSC analyses. The Institute of Organic Chemistry (TU-Clausthal) is acknowledged for performing the NMR analyses.

Author Contributions: The PVDF synthesis in supercritical CO_2 , the synthesis of the block copolymers, FT-IR and AFM measurements were carried out by Nahal Golzari. Jörg Adams performed the XRD analyses at TU Clausthal. The manuscript was prepared by Nahal Golzari, Jörg Adams, and Sabine Beuermann.

Conflicts of Interest: The authors declare no conflict of interest.

References

1. Humphrey, J.S.; Amin-Sanayei, R. Vinylidene Fluoride Polymers. In *Encyclopedia of Polymer Science and Technology*, 3rd ed.; Wiley: New York, NY, USA, 2002; pp. 510–533.
2. Scheirs, J. *Modern Fluoropolymers: High Performance Polymers for Diverse Applications*; Wiley: Chichester, UK; New York, NY, USA, 1997; ISBN 978-0-471-97055-2.
3. Ameduri, B. From Vinylidene Fluoride (VDF) to the Applications of VDF-Containing Polymers and Copolymers: Recent Developments and Future Trends. *Chem. Rev.* **2009**, *109*, 6632–6686. [[CrossRef](#)] [[PubMed](#)]
4. Beuermann, S.; Imran-ul-haq, M. Homogeneous phase polymerization of vinylidene fluoride in supercritical CO₂: Surfactant free synthesis and kinetics. *Macromol. Symp.* **2007**, *259*, 210–217. [[CrossRef](#)]
5. Lu, F.J.; Hsu, S.L. Study of the crystallization behavior of poly(vinylidene fluoride) from melt under the effect of an electric field. *Macromolecules* **1986**, *19*, 326–329. [[CrossRef](#)]
6. Kawai, H. The Piezoelectricity of Poly(vinylidene fluoride). *Jpn. J. Appl. Phys.* **1969**, *8*, 975–976. [[CrossRef](#)]
7. Bergman, J.G., Jr.; Mcfee, J.H.; Crane, G.R. Pyroelectricity and optical second harmonic generation in poly(vinylidene fluoride) films. *Appl. Phys. Lett.* **1971**, *18*, 203. [[CrossRef](#)]
8. Nakamura, K.; Wada, Y. Piezoelectricity, pyroelectricity, and the electrostriction constant of poly(vinylidene fluoride). *J. Polym. Sci. Part B Polym. Phys.* **1971**, *9*, 161–173. [[CrossRef](#)]
9. Lovinger, A.J. Molecular Mechanism for α (δ Transformation in Electrically Poled Poly(vinylidene fluoride)). *Macromolecules* **1981**, *14*, 225–227. [[CrossRef](#)]
10. Kepler, R.G. *Ferroelectric, Pyroelectric, and Piezoelectric Properties of Poly(vinylidene fluoride) in Ferroelectric Polymers Chemistry, in Physics and Applications*; Nalwa, H.S., Ed.; CRC Press: New York, NY, USA, 1995; p. 183, ISBN 0-8247-9468-0.
11. Hasegawa, R.; Kobayashi, M.; Tadokoro, H. Molecular conformation and packing of poly(vinylidene fluoride). Stability of three crystalline forms and the effect of high pressure. *Polym. J.* **1972**, *3*, 591–599. [[CrossRef](#)]
12. Lovinger, A.; Reed, D. Inhomogeneous Thermal Degradation of Poly(vinylidene fluoride) Crystallized from the Melt. *Macromolecules* **1980**, *13*, 989–994. [[CrossRef](#)]
13. Martins, P.; Lopes, A.C.; Lanceros-Mendez, S. Electroactive phases of poly(vinylidene fluoride): Determination, processing and applications. *Prog. Polym. Sci.* **2014**, *39*, 683–706. [[CrossRef](#)]
14. Fukada, E. History and recent progress in piezoelectric polymers. *IEEE Trans. Ultrason. Ferroelectr. Freq. Control* **2000**, *47*, 1277–1290. [[CrossRef](#)] [[PubMed](#)]
15. Bauer, F. Relaxor fluorinated polymers: Novel applications and recent developments. *IEEE Trans. Dielectr. Electr. Insul.* **2010**, *17*, 1106–1112. [[CrossRef](#)]
16. Jungnickel, B.J. PVDF and Its Blends. In *Ferroelectric Polymers Chemistry, in Physics and Applications*; Nalwa, H.S., Ed.; CRC Press: New York, NY, USA, 1995; p. 183, ISBN 0-8247-9468-0.
17. Valade, D.; Boyer, C.; Ameduri, B.; Boutevin, B. Poly(vinylidene fluoride)-*b*-poly(styrene) Block Copolymers by Iodine Transfer Polymerization (ITP): Synthesis, Characterization, and Kinetics of ITP. *Macromolecules* **2006**, *39*, 8639–8651. [[CrossRef](#)]
18. Boutevin, B. From telomerization to living radical polymerization. *J. Polym. Sci. Part A Polym. Chem.* **2000**, *38*, 3235–3243. [[CrossRef](#)]
19. David, G.; Boyer, C.; Tonnar, J.; Ameduri, B.; Lacroix-Desmazes, P.; Boutevin, B. Use of Iodocompounds in Radical Polymerization. *Chem. Rev.* **2006**, *106*, 3936–3962. [[CrossRef](#)] [[PubMed](#)]
20. Boyer, C.; Valade, D.; Sauguet, L.; Ameduri, B.; Boutevin, B. Iodine Transfer Polymerization (ITP) of Vinylidene Fluoride (VDF). Influence of the defect of VDF chaining on the control of ITP. *Macromolecules* **2005**, *38*, 10353–10362. [[CrossRef](#)]
21. Girard, E.; Marty, J.D.; Ameduri, B.; Destarac, M. Direct synthesis of Vinylidene Fluoride-Based Amphiphilic Diblock Copolymers by RAFT/MADIX Polymerization. *ACS Macro Lett.* **2012**, *1*, 270–274. [[CrossRef](#)]
22. Guerre, M.; Campagne, B.; Gimello, O.; Parra, K.; Ameduri, B.; Ladmiral, V. Deeper Insight into the MADIX Polymerization of Vinylidene Fluoride. *Macromolecules* **2015**, *48*, 7810–7822. [[CrossRef](#)]
23. Guerre, M.G.; Lopez, T.; Soulestin, C.; Totée, B.; Améduri, G.; Silly, V.; Ladmiral, A. Journey into the Microstructure of PVDF Made by RAFT. *Macromol. Chem. Phys.* **2016**, *217*, 2275–2285. [[CrossRef](#)]

24. Monteiro, M.J.; Adamy, M.M.; Leeuwen, B.J.; van Herk, A.M.; Destarac, M. A “Living” Radical ab Initio Emulsion Polymerization of Styrene Using a Fluorinated Xanthate Agent. *Macromolecules* **2005**, *38*, 1538–1541. [[CrossRef](#)]
25. Guerre, M.; Schmidt, J.; Talmon, Y.; Ameduri, B.; Ladmiral, V. An amphiphilic poly(vinylidene fluoride)-*b*-poly(vinyl alcohol) block copolymer: Synthesis and self-assembly in water. *Polym. Chem.* **2017**, *8*, 1125–1128. [[CrossRef](#)]
26. Guerre, M.; Uchiyama, M.; Folgado, E.; Semsarilar, M.; Ameduri, B.; Satoh, K.; Kamigato, M.; Ladmiral, V. Combination of Cationic and Radical RAFT Polymerizations: A Versatile Route to Well-Defined Poly(ethyl vinyl ether)-block-poly(vinylidene fluoride) Block Copolymers. *ACS Macro Lett.* **2017**, *6*, 393–398. [[CrossRef](#)]
27. Boyer, C.; Valade, D.; Lacroix-Desmazes, P.; Ameduri, B.; Boutevin, B. Kinetics of the Iodine Transfer Polymerization of Vinylidene Fluoride. *J. Polym. Sci. Part A Polym. Chem.* **2006**, *44*, 5763–5777. [[CrossRef](#)]
28. Vukićević, R.; Vukovic, I.; Stoyanov, H.; Korwitz, A.; Pospiech, D.; Kofod, G.; Loos, K.; Brinke, G.; Beuermann, S. Poly(vinylidene fluoride)-functionalized single-walled carbon nanotubes for the preparation of composites with improved conductivity. *Polym. Chem.* **2012**, *3*, 2261–2265. [[CrossRef](#)]
29. Vukićević, R.; Hirzenberger, P.; Hild, S.; Beuermann, S. Functionalization of carbon black nanoparticles with poly(vinylidene fluoride). *J. Polym. Sci. Part A Polym. Chem.* **2010**, *48*, 4847–4854. [[CrossRef](#)]
30. Vukićević, R.; Schwadtke, U.; Schmücker, S.; Schäfer, P.; Kuckling, D.; Beuermann, S. Alkyne-azide coupling of tailored poly(vinylidene fluoride) and polystyrene for the synthesis of block copolymers. *Polym. Chem.* **2012**, *3*, 409–414. [[CrossRef](#)]
31. Asandei, A.D.; Adebolu, O.I.; Simpson, C.P. Mild-Temperature Mn₂(CO)₁₀-Photomediated Controlled Radical Polymerization of Vinylidene Fluoride and Synthesis of Well-Defined Poly(vinylidene fluoride) Block Copolymers. *J. Am. Chem. Soc.* **2012**, *134*, 6080–6083. [[CrossRef](#)] [[PubMed](#)]
32. Simpson, C.P.; Adebolu, O.I.; Kim, J.-S.; Vasu, V.; Asandei, A.D. Metal and Ligand Effects of Photoactive Transition Metal Carbonyls in the Iodine Degenerative Transfer Controlled Radical Polymerization and Block Copolymerization of Vinylidene Fluoride. *Macromolecules* **2015**, *48*, 6404–6420. [[CrossRef](#)]
33. Asandei, A.D. Photomediated Controlled Radical Polymerization and Block Copolymerization of Vinylidene Fluoride. *Chem. Rev.* **2016**, *116*, 2244–2247. [[CrossRef](#)] [[PubMed](#)]
34. Rowlands, G.J. Radicals in organic synthesis. Part 1. *Tetrahedron* **2009**, *65*, 8603–8655. [[CrossRef](#)]
35. Goodman, J.L.; Peters, K.S.; Vaida, V. The Determination of the Mn-Mn Bond Strength in Mn₂(CO)₁₀ Using Pulsed Time Resolved Photoacoustic Calorimetry. *Organometallics* **1986**, *5*, 815–816. [[CrossRef](#)]
36. Sarakha, M.; Ferraudi, G. Photophysical Features of the M₂(CO)₁₀, M = Mn and Re, Solution Photochemistry. *Inorg. Chem.* **1999**, *38*, 4605–4607. [[CrossRef](#)] [[PubMed](#)]
37. Voet, V.S.D.; Hermida-Merino, D.; ten Brinke, G.; Loos, K. Block copolymer route towards poly(vinylidene fluoride)/poly(methacrylic acid)/nickel nanocomposites. *RSC Adv.* **2013**, *3*, 7938–7946. [[CrossRef](#)]
38. Voet, V.S.D.; Alberda van Ekenstein, G.O.R.; Meereboer, N.L.; Hofman, A.H.; ten Brinke, G.; Loos, K. Double-crystalline PLLA-*b*-PVDF-*b*-PLLA triblock copolymers: Preparation and crystallization. *Polym. Chem.* **2014**, *5*, 2219–2230. [[CrossRef](#)]
39. Voet, V.S.D.; Tichelaar, M.; Tanase, S.; Mittelmeijer-Hazeleger, M.C.; ten Brinke, G.; Loos, K. Poly(vinylidene fluoride)/nickel nanocomposites from semicrystalline block copolymer precursors. *Nanoscale* **2013**, *5*, 184–192. [[CrossRef](#)] [[PubMed](#)]
40. Beuermann, S.; Imran-ul-haq, M. Homogeneous Phase Polymerization of Vinylidene Fluoride in Supercritical Carbon Dioxide. *J. Polym. Sci. Part A Polym. Chem.* **2007**, *45*, 5626–5635. [[CrossRef](#)]
41. Möller, E.; Beuermann, S. Homogeneous Phase Copolymerizations of Vinylidene Fluoride and Hexafluoropropene in Supercritical Carbon Dioxide. *Macromol. React. Eng.* **2011**, *5*, 8–21. [[CrossRef](#)]
42. Brandl, F.; Beuermann, S. Halb-kontinuierliche Emulsionspolymerisation von Vinylidenfluorid. *Chem. Ing. Tech.* submitted.
43. Nick, L.; Kindermann, A.; Fuhrmann, J. Morphological studies of spin-coated films of poly(styrene-block-methyl methacrylate) copolymers by atomic force microscopy. *Colloid Polym. Sci.* **1994**, *272*, 367–371. [[CrossRef](#)]
44. Gallot-Grubisic, Z.; Rempp, P.; Benoit, H.J. A universal calibration for gel permeation chromatography. *Polym. Sci. Part B Polym. Lett.* **1967**, *5*, 753–759. [[CrossRef](#)]
45. Siegmann, R.; Drache, M.; Beuermann, S. Propagation rate coefficients for vinylidene fluoride homopolymerizations. *Macromolecules* **2013**, *46*, 9507–9514. [[CrossRef](#)]

46. Guiot, J.; Ameduri, B.; Boutevin, B. Radical Homopolymerization of Vinylidene Fluoride Initiated by *tert*-Butyl Peroxypivalate. Investigation of the Microstructure by ^{19}F and ^1H NMR Spectroscopies and Mechanisms. *Macromolecules* **2002**, *35*, 8694–8707. [[CrossRef](#)]
47. Balague, J.; Ameduri, B.; Boutevin, B.; Caporiccio, G. Controlled step-wise telomerization of vinylidene fluoride, hexafluoropropene and trifluoroethylene with iodofluorinated transfer agents. *J. Fluor. Chem.* **2000**, *102*, 253–268. [[CrossRef](#)]
48. Hesse, M.; Meier, H.; Zeeh, B. *Spektroskopische Methoden in der Organischen Chemie*, 7th ed.; Thieme: Stuttgart, Germany, 2005.
49. Paul, D.R.; Altamirano, J.O. Properties of compatible blends of poly(vinylidene fluoride) and poly(methyl methacrylate). *Adv. Chem. Ser.* **1975**, *142*, 371–385. [[CrossRef](#)]
50. Noland, J.S.; Hsu, N.N.; Schmitt, J.M. Compatible high polymers: Poly(vinylidene fluoride) blends with homopolymers of methyl and ethyl methacrylate. *Adv. Chem. Ser.* **1971**, *99*, 15–28. [[CrossRef](#)]
51. Yano, S. Dielectric relaxation and molecular motion in poly(vinylidene fluoride). *J. Polym. Sci. Part B Polym. Phys.* **1970**, *8*, 1057–1072. [[CrossRef](#)]
52. Kakutani, H. Dielectric absorption in oriented poly(vinylidene fluoride). *J. Polym. Sci. Part B Polym. Phys.* **1970**, *8*, 1177–1186. [[CrossRef](#)]
53. Li, P.; Maier, J.M.; Vik, E.C.; Yehl, C.J.; Dial, B.E.; Rickher, A.E.; Smith, M.D.; Pellechia, P.J.; Shimizu, K.D. Stabilizing Fluorine— π Interactions. *Angew. Chem. Int. Ed.* **2017**, *56*, 7209–7212. [[CrossRef](#)] [[PubMed](#)]
54. Hunter, L. The C-F bond as a conformational tool in organic and biological chemistry. *Beilstein J. Org. Chem.* **2010**, *6*, 38. [[CrossRef](#)] [[PubMed](#)]
55. O'Hagan, D. Understanding organofluorine chemistry. An introduction to the C-F bond. *Chem. Soc. Rev.* **2008**, *37*, 308–319. [[CrossRef](#)] [[PubMed](#)]
56. Hof, F.; Scofield, D.M.; Schweizer, W.B.; Diederich, F. A weak attractive interaction between organic fluorine and an amide group. *Angew. Chem. Int. Ed.* **2004**, *43*, 5056–5059. [[CrossRef](#)] [[PubMed](#)]



© 2017 by the authors. Licensee MDPI, Basel, Switzerland. This article is an open access article distributed under the terms and conditions of the Creative Commons Attribution (CC BY) license (<http://creativecommons.org/licenses/by/4.0/>).